Journal of Statistical Physics, Vol. 69, Nos. 1/2, 1992

Free Fermion Approximation for the Ising Model with Further-Neighbor Interactions on a Triangular Lattice

A. Kooiman[1] **and J. M. J. van Leeuwen**[1]

Received January 23, 1992

The free fermion solution/approximation for the Ising model on a triangular lattice with further-neighbor interactions is derived, using Vdovichenko's method. For isotropic first- and second-neighbor interactions K, $L \geqslant 0$, the approximation is a strict lower bound for the partition sum. We have also obtained the approximate critical surface, where the critical behavior is Ising-like, and the exact zero-temperature phase diagram when the interactions are isotropic. A recent extension of the method of Vdovichenko due to Calheiros *et al.* makes it easy to give the surface free energy and the equilibrium crystal shape as well, in the ferromagnetic regime and for a regime where the phase is ordered in layers.

KEY WORDS: Vertex pairs; topological theorem; graphs; paths.

INTRODUCTION

Since Onsager's solution of the 2D Ising model[1] many efforts have been made to extend the solution to include further-neighbor interactions. Such solutions would allow for a better modeling of real magnetic systems[2] and of course of all other systems that can be mapped onto the Ising model such as, e.g., recent models for microemulsions.[3,4] The only generalizations along this line that have led to exact solutions are the free fermion models (models that can be rewritten as free fermion field theories[5]), where still certain restrictions have to be imposed on the values allowed for the coupling constants. But for a large range of values where these conditions are not met, simply ignoring them still provides a good approximation to the real solution (the so-called free fermion approximation[6]).

[1] Instituut-Lorentz, 2311 SB Leiden, The Netherlands.

0022-4715/92/1000-0247$06.50/0

Of the different methods that can be employed to solve these models, Vdovichenko's method[7-10] has the advantage that it can easily be extended to yield the surface tension[11-13] as well as the corresponding equilibrium crystal shape.[12,13]

In this paper we present the free fermion solution/approximation for the Ising model with first- and second-neighbor interactions and a four-spin interaction on a triangular lattice, using the method of Vdovichenko.[8] In Section 1 we define the model and rewrite it as a vertex-pair model on the dual lattice. The zero-temperature phase diagram of the isotropic model is given in Section 2. In Section 3 we derive the free fermion conditions for which the solution will be exact and in Section 4 we calculate the, in general approximate, partition sum and discuss the accuracy of the approximation. The approximate critical surface of the model is derived in Section 5 and in Section 6 we study the surface free energy.

1. THE MODEL

Consider a triangular lattice consisting of N sites with periodic boundary conditions. On every site there is an Ising spin $\sigma = \pm 1$. Any two neighboring elementary triangles of the lattice form a diamond. To each diamond we assign three interactions (see Fig. 1), a first- and second-neighbor interaction K_i and L_i (along the two diagonals of the diamond) and a four-spin interaction Q_i, $i = 1$, 2, or 3. In the interaction constants we have already absorbed a factor $1/k_B T$ for later convenience. Note that each triangle is part of three diamonds (the diamonds overlap), one in each possible orientation. For each of the three orientations i a diamond can occur in eight different configurations q, depicted in Fig. 2. The energy E of a configuration of the system is given by

$$E = \sum_{i=1}^{3} \sum_{q=1}^{8} n_i(q)\, \varepsilon_i(q) \tag{1.1}$$

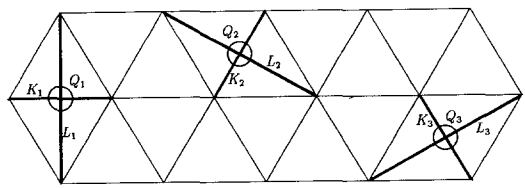

Fig. 1. The lattice is seen as built up out of overlapping diamonds. We assign to each diamond a first- and second-neighbor interaction and a four-spin interaction, with coupling constants K_i, L_i, and Q_i, respectively, whose values are different for each orientation i.

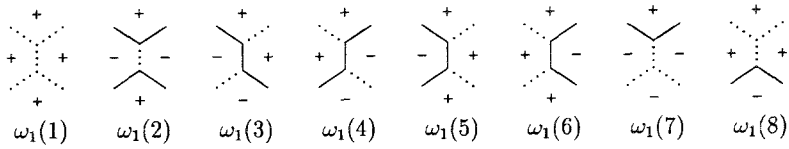

Fig. 2. A diamond on the original lattice corresponds to a vertex pair on the dual lattice. The figure shows all possible configurations $q = 1,..., 8$ for a vertex pair in orientation 1, together with their weights $\omega_1(q)$.

where

$$\varepsilon_i(q) = -(K_i\sigma_1\sigma_3 + L_i\sigma_2\sigma_4 + Q_i\sigma_1\sigma_2\sigma_3\sigma_4) \tag{1.2}$$

is the energy of a diamond of type (i, q), and $n_i(q)$ is the number of times this diamond occurs in the configuration.

Thus the partition sum becomes

$$Z = \sum_{\{\text{configurations}\}} \sum_{i=1}^{3} \sum_{q=1}^{8} [\omega_i(q)]^{n_i(q)} \tag{1.3}$$

with

$$\omega_i(q) = \exp[-\varepsilon_i(q)] \tag{1.4}$$

The partition sum is invariant under the following transformation. Reverse all spins on every other line parallel to one of three principal axes and combine it with a change of sign of the coupling constants K and L in the other two directions. Hence we have

$$\begin{aligned} &Z(K_1, K_2, K_3, L_1, L_2, L_3, Q_1, Q_2, Q_3) \\ &\quad = Z(-K_1, -K_2, K_3, -L_1, -L_2, L_3, Q_1, Q_2, Q_3) \qquad (1.5) \\ &\quad = Z(-K_1, K_2, -K_3, -L_1, L_2, -L_3, Q_1, Q_2, Q_3) \qquad (1.6) \\ &\quad = Z(K_1, -K_2, -K_3, L_1, -L_2, -L_3, Q_1, Q_2, Q_3) \qquad (1.7) \end{aligned}$$

The model is equivalent to a vertex-pair model on the dual (hexagonal) lattice.[14] In the dual language the configurations are specified by placing bonds between nearest neighbor sites of the dual lattice, separating unequal spins on the original lattice (see Fig. 3). Only 0 or 2 bonds meet at every dual lattice site, forming closed loops that cannot cross. A set of loops belonging to one configuration is called a graph. When there is no bond between two nearest-neighbor sites on the dual lattice, we speak of a hole.

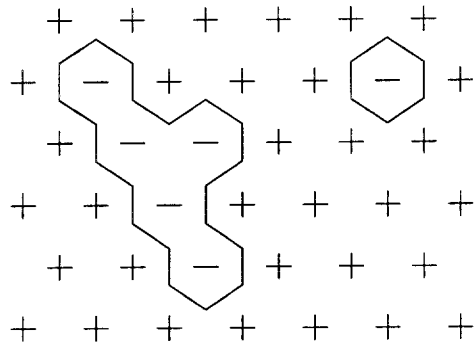

Fig. 3. In the dual language configurations are specified by drawing lines on the dual lattice separating unequal spins on the original lattice. At every lattice site, 2 or 0 line elements (called bonds) meet.

To every diamond on the triangular lattice there corresponds a vertex pair on the dual lattice (see Fig. 2). In Appendix A we derive all independent relations that exist between the numbers $n_i(q)$ and show that, as a result, the partition sum can be rewritten as

$$Z=[\omega_1(1)\,\omega_2(1)\,\omega_3(1)]^N \sum_{\{\text{configurations}\}} \prod_{i=1}^{3} a_i^{n_i(2)} b_i^{n_i(5)+n_i(6)} c_i^{n_i(7)+n_i(8)} \tag{1.8}$$

with

$$a_i=\frac{\omega_i(2)\,\omega_{i+1}(3)\,\omega_{i+2}(4)}{\omega_i(1)\,\omega_{i+1}(1)\,\omega_{i+2}(1)} \tag{1.9}$$

$$b_i=\left(\frac{\omega_i(5)\,\omega_i(6)}{\omega_i(3)\,\omega_i(4)}\right)^{1/2} \tag{1.10}$$

$$c_i=\left(\frac{\omega_i(7)\,\omega_i(8)\,\omega_{i+1}(3)\,\omega_{i+2}(4)}{[\omega_i(1)]^2\,\omega_{i+1}(1)\,\omega_{i+2}(1)}\right)^{1/2} \tag{1.11}$$

and $i=i \pmod 3$.

For the application of the method of Vdovichenko, a more appropriate formulation of the partition sum is[8]

$$Z=\left[\prod_i^3 \omega_i(1)\right]^N \sum_G I_G \tag{1.12}$$

where the sum is over all graphs G on the dual lattice and I_G, the Boltzmann weight of the configuration specified by graph G, is given by

$$\begin{aligned} I_G &= \prod_{i=1}^{3} a_i^{n_i(2)} b_i^{n_i(5)+n_i(6)} c_i^{n_i(7)+n_i(8)} \\ &= \prod_{i=1}^{3} c_i^{n_{c_i}} b_i^{n_{b_i}} x_i^{n_{x_i}} \end{aligned} \tag{1.13}$$

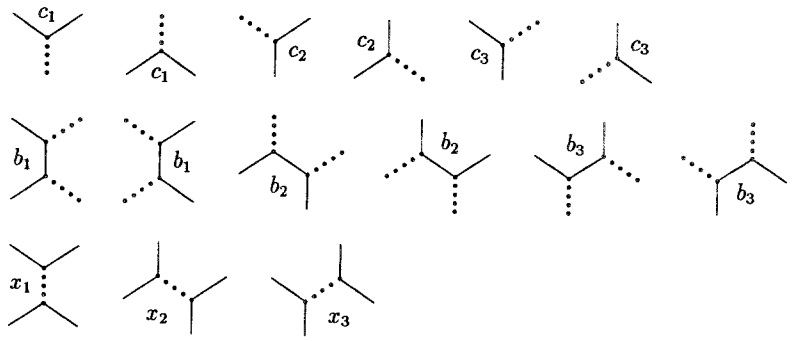

Fig. 4. Weights assigned to corners, bends, and close encounters.

with the weight

$$x_i = \frac{a_i}{c_i^2} = \frac{\omega_i(1)\,\omega_i(2)}{\omega_i(7)\,\omega_i(8)} \tag{1.14}$$

and

$$n_{c_i} = 2n_i(2) + n_i(7) + n_i(8) \tag{1.15}$$

the total number of corners (single turns) with orientation i in graph G, to each of which a weight c_i is assigned,

$$n_{b_i} = n_i(5) + n_i(6) \tag{1.16}$$

the total number of bends (two successive turns in the same direction) with orientation i in graph G, to each of which a weight b_i is assigned, and

$$n_{x_i} = n_i(2) \tag{1.17}$$

the total number of close encounters with orientation i in graph G, to each of which a weight x_i is assigned (see Fig. 4). The factor in front of the sum rescales I_G so that $I_G = 1$ for $G = \varnothing$ (the empty graph representing the configuration with all spins parallel). As an example, the Boltzmann weight for the graph in Fig. 5 is given by

$$I_G = c_1^6 c_2^2 c_3^2 b_1^2 b_2^2 b_3^2 x_1 \tag{1.18}$$

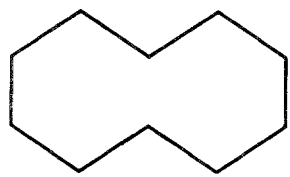

Fig. 5. An example of a graph. The Boltzmann weight of this graph is given by $I_G = c_1^6 c_2^2 c_3^2 b_1^2 b_2^2 b_3^2 x_1$.

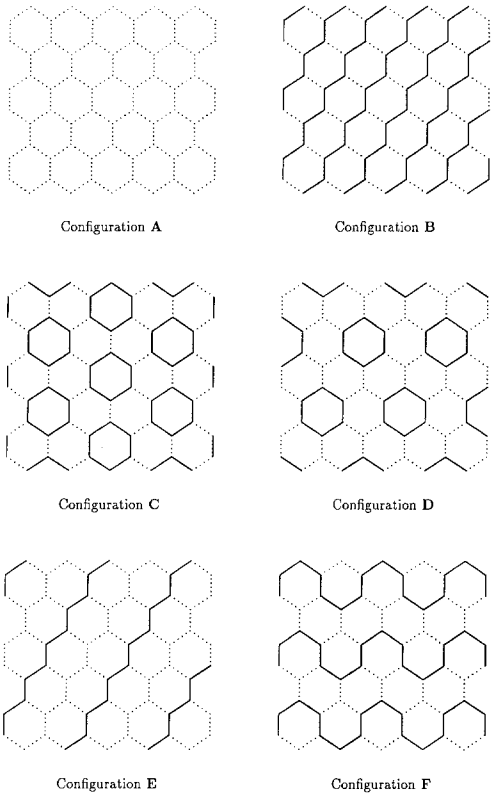

Fig. 6. The ground states for the isotropic model.

Expressing the corner, bend, and close encounter weights in the original language of coupling constants, using Eqs. (1.2) and (1.4), we obtain

$$c_i = \exp[-2(L_i + Q_i) - (K_{i+1} + L_{i+1} + K_{i+2} + L_{i+2})] \tag{1.19}$$

$$b_i = \exp[2(L_i - Q_i)] \tag{1.20}$$

$$x_i = \exp[4(L_i + Q_i)] \tag{1.21}$$

For the nearest-neighbor Ising model, the coupling constants L_i and Q_i are zero, so that $c_i = \exp(-K_{i+1} - K_{i+2})$ and $x_i = b_i = 1$ for $i = 1, 2, 3$.

2. THE ZERO-TEMPERATURE PHASE DIAGRAM

The ground state for arbitrary coupling constants may be very complicated since the various tendencies compete and disorder can exist down to zero temperature. Therefore we restrict ourselves to the isotropic case: $K_i = K$, $L_i = L$, and $Q_i = Q$ for $i = 1, 2, 3$. A superficial inspection readily shows that the configurations A–F as shown in Fig. 6 are the ground states in some part of the phase diagram. Since the energies of the configurations are given by

$$\begin{aligned} E_A &= -N \ln\left[\prod_i^3 \omega_i(1)\right] \\ E_B &= E_A - N \ln(c^2 x) \\ E_C &= E_A - N \ln(b^2 c^2 x) \\ E_D &= E_A - (3N/2) \ln(bc) \\ E_E &= E_A - N \ln(c) \\ E_F &= E_A - (N/2) \ln(b^2 c^3) \end{aligned} \tag{2.1}$$

we can also find the domains for these ground states, if they are the only contenders. In Figs. 7 and 8 we give these domains for $Q > 0$ and $Q < 0$.

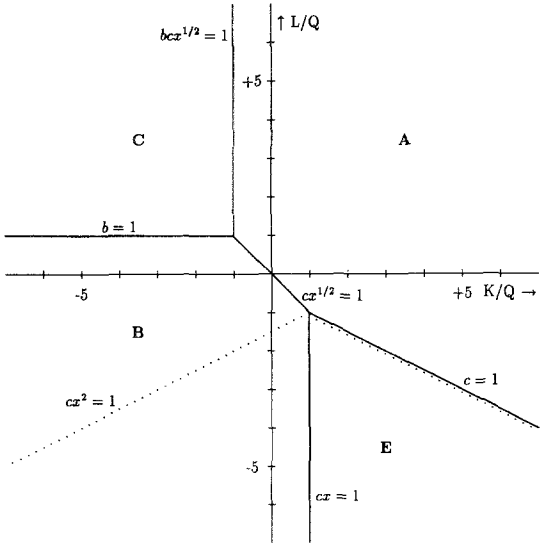

Fig. 7. The zero-temperature phase diagram for the isotropic model with $Q > 0$. The letter A, B, C, and E refer to the ground states as given in Fig. 6. The boundary equations follow from equating their weights.

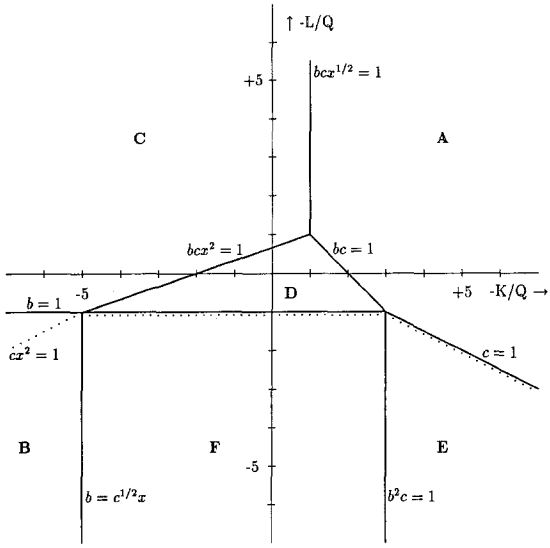

Fig. 8. The zero-temperature phase diagram for the isotropic model with $Q < 0$. The letters A–F refer to the ground states as given in Fig. 6.

We prove in Appendix B that the ground states A–E are indeed the ground states of the system in their domain. For state F the arguments presented are not sufficient to rule out possible other states as ground states. We indicate why we find it plausible that F is indeed the ground state in its domain. We have not further investigated this case, since it involves an examination of the lattice on a larger scale than a hexagon (which is sufficient for A–E) and since the free fermion approximation is inaccurate in this region of the phase diagram anyway.

3. THE FREE FERMION CONDITIONS

A graph consists of a number of closed loops. These loops are not independent, because they avoid each other and because weights are assigned to close encounters. When $x_i = b_i = 1$ (the nearest-neighbor Ising model) the loops can be made independent by a trick. This can be expressed in the form of a topological theorem, which was first conjectured by Feynman[7] and later proven by Sherman[15,16]:

$$\sum_G I_G = \prod_p (1 + W_p) \tag{3.1}$$

On the left-hand side (lhs) we have essentially the partition sum of Eq. (1.12), while on the right-hand side (rhs) there is a product over all

closed nonperiodic paths p (any closed nonperiodic trajectory that can be traced out by a random walker). W_p, the weight of path p, is given by

$$W_p = (-1)^{n_p} I_p = -(-1)^{t_p} I_p \tag{3.2}$$

with n_p the number of self-crossings, t_p the winding number, and I_p the Boltzmann weight of path p. Similar to Eq. (1.13) we have ($x_i = b_i = 1$)

$$I_p = \prod_{i=1}^{3} c_i^{n_{c_i}} \tag{3.3}$$

with n_{c_i} the number of times c_i occurs in path p. Note that the set of paths is much larger than the set of loops, because self-overlap is allowed and because expanding the rhs of the topological theorem also generates products of paths that partly overlap. The sum of all terms (=products of paths) *without* overlapping bonds gives exactly the lhs of Eq. (3.1). So all other terms in the expansion must cancel. The sign introduced in the path weights takes care of that.[7,16] This is the trick that decouples the paths and because the sign is determined by the winding number, it can be locally implemented by assigning a proper phase factor $\exp(\pm i\pi/6)$ to each turn in the path. The topological theorem is the foundation on which the whole method of Vdovichenko is based.

Thus the method of Vdovichenko replaces the sum over graphs by a sum over products of independent paths. For our model, two complications arrise in this crucial step. First, it is evident that in the path weights no close encounter weights $x_i \neq 1$ may occur, otherwise the path cannot be interpreted as a random walker trajectory with local transition probabilities. Therefore we put for the Boltzmann weight of path p

$$I_p = \prod_{i=1}^{3} b_i^{n_{b_i}} c_i^{n_{c_i}} \tag{3.4}$$

where the close encounter weights x_i have been left out. Second, when the bend weight $b_i \neq 1$, the trick above does not give a complete cancellation of all additional terms in the expansion of the rhs of Eq. (3.1). In Appendix C we show that all terms with an overlap consisting solely of a number of occurrences of the bond configurations, depicted in Fig. 9, do

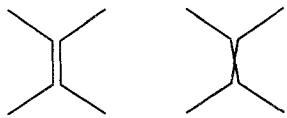

Fig. 9. The two new bond configurations for a vertex pair that arise when working out the product over paths in the topological theorem (considering only the terms that do not cancel).

not cancel. So it appears that the topological theorem cannot be used for a wider class than the nearest-neighbor Ising model. But we will show below that the contributions from the additional paths can be interpreted as close encounter weights in the graphs and that under certain restrictions the topological theorem is exact even when x_i, $b_i \neq 1$ (the two mistakes exactly compensate one another).

We will now try to establish the conditions under which the topological theorem is valid. It is customary to speak of them as free fermion conditions because, when they apply, the model is equivalent to a free fermion field theory.[5,6] Consider the diagram equation in Fig. 10. If in all graphs on the lhs of Eq. (3.1), each close encounter is replaced by the sum of the three diagrams, shown on the rhs of the diagram equation, then all surviving terms of the rhs of Eq. (3.1) are generated. So, if there are k close encounters in a graph, there are 3^k corresponding paths and the sum of their weights must be made equal to that of the graph. When the close encounters have no bonds in common, we can do this by restricting the close encounter weights in the graph in accordance with the diagram equation of Fig. 10:

$$c_i^2 x_i = c_i^2 + b_{i+1}^{\mu_i} b_{i+2}^{\nu_i} (c_{i+1}^2 c_{i+2}^2 b_i^2 - c_{i+1}^2 c_{i+2}^2) \tag{3.5}$$

with μ_i, $\nu_i = 0, \pm 2$ for $i = 1, 2, 3$. On the lhs we have the factor that the diagram on the lhs of the diagram equation contributes to the graph weight. Similarly, the three terms on the rhs are the factors that the corresponding diagrams on the rhs of the diagram equation contribute to the path weights. In the term on the lhs there are two corner weights and a weight for the close encounter (only in the path weights are close encounter weights left out, not in the graphs). The first term on the rhs is c_i^2 because the close encounter weight x_i cannot be incorporated in the path weights. The common factor $b_{i+1}^{\mu_i} b_{i+2}^{\nu_i}$ in the last two terms arises because the two extra bonds make bends appear/disappear (for each outward bond there is an exchange, bend $\leftrightarrow$ no bend, because one of its neighboring bonds has

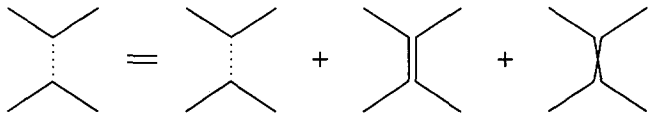

Fig. 10. The two new vertex pair configurations as given in Fig. 9 can be considered as two additional path interpretations of a close encounter. The weight of a close encounter in a graph should be choosen equal to the sum of the weights of the three path interpretations of this close encounter, i.e., the diagram equation in this figure must hold (when close encounters have no bonds in common).

changed its direction). The minus sign in the last term is due to the extra bond crossing in the last diagram. So we obtain the free fermion conditions

$$x_i = 1 + b_{i+1}^{\mu_i} b_{i+2}^{\nu_i} z_i, \qquad \mu_i, \nu_i = 0, \pm 2 \tag{3.6}$$

with

$$z_i = \left(\frac{c_{i+1} c_{i+2}}{c_i} \right)^2 (b_i^2 - 1) \tag{3.7}$$

When two close encounters share a bond (see Fig. 11), they interfere with each other. For instance, for the first diagram in Fig. 11 we have [similar to Eq. (3.6)]

$$x_1 x_3 = 1 + b_2^{\mu_1} b_3^{\nu_1} z_1 + b_1^{\mu_2} b_2^{\nu_2} z_3 + b_1^{\mu_2} b_2^{\mu_1 + \nu_2 + 2} b_3^{\nu_1} z_1 z_3 \tag{3.8}$$

with $\mu_1, \nu_2 = 0, \pm 2$ and $\mu_2, \nu_1 = -2, 0$. In the last term, the exponent of b_2 has an extra 2 because, if both close encounters change to a double bond configuration, the bond shared by the close encounters makes no exchange, bend $\leftrightarrow$ no bend. Therefore the equation does not factorize into two equations with forms similar to that of Eq. (3.6). In this way, for every group of close encounters lumping together, new free fermion conditions will be found. In spite of all these complications, there exists a nontrivial solution. If we choose one direction as special (say direction i) and for the other two directions set

$$b_{i+1} = b_{i+2} = 1 \tag{3.9}$$

Eq. (3.6) becomes

$$x_i = 1 + z_i, \qquad x_{i+1} = x_{i+2} = 1 \tag{3.10}$$

and all other free fermion conditions do factorize into products of Eq. (3.10), leaving a total of only five restrictions which can be satisfied in

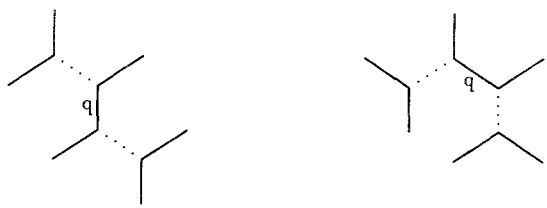

Fig. 11. Diagrams with two close encounters that have a bond (bond q) in common.

a nontrivial way. Translating Eqs. (3.9) and (3.10) back to the Ising language with Eqs. (1.19)–(1.21), we obtain

$$L_{i+1} = L_{i+2} = Q_{i+1} = Q_{i+2} = 0 \tag{3.11}$$

and

$$\exp(-4Q_i) = \frac{\cosh[2(K_i + L_i)]}{\cosh[2(K_i - L_i)]} \tag{3.12}$$

These are the free fermion conditions under which the topological theorem is valid. They reduce the model to the free fermion model on a square lattice, as studied by Fan and Wu[6] (see Fig. 12). The nonzero coupling constants should be renamed as follows:

$$\begin{aligned} K &= K_{i+1}, \qquad L = K_i, \qquad Q = Q_i \\ K' &= K_{i+2}, \qquad L' = L_i \end{aligned} \tag{3.13}$$

In the dual language it means that the central bond of the vertex pairs, depicted in Fig. 2, should be shrunk to a point [since they no longer correspoond to a nearest neighbor interaction $(K_i = L)$], so that the vertex pairs transform into the vertices of the eight-vertex model. Equation (3.12) can also be written as

$$\omega_i^{(1)}\omega_i^{(2)} + \omega_i^{(3)}\omega_i^{(4)} = \omega_i^{(5)}\omega_i^{(6)} + \omega_i^{(7)}\omega_i^{(8)} \tag{3.14}$$

which is the more usual form for the free fermion condition for this model.

What are the results so far? There are no free fermion solutions in our model, other then the ones already found for the square lattices. But if the

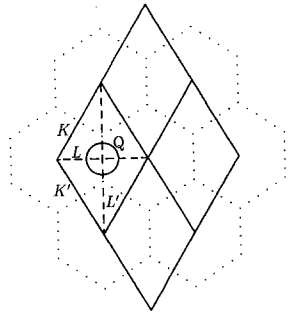

Fig. 12. When Eq. (3.11) holds and we rename the other coupling constants as in (3.13), the model is equivalent to the eight-vertex model on a square lattice as shown in the figure for $i = 1$.

free fermion conditions are not met, wrong weights are given only to the close encounters in the graphs. So for any set of values of variables c_i, b_i, and x_i we can give an approximate solution that fully takes into account the corner- and the bend-weights, while the close encounter weights, as dictated by the free fermion conditions (3.6), are in general different form the real close encounter weights given by Eq. (1.21). When the coupling constants are such (as in the ferromagnetic phase at low temperatures) that close encounters are rare, the result will be a good approximation (the free fermion approximation).

4. THE FREE FERMION SOLUTION/APPROXIMATION

We will now continue with the weight (3.4) and use Eq. (3.1). On the basis of Eq. (3.1) it is easy to evaluate the partition sum. It is exact only when the topological theorem is exact, that is, when the free fermion conditions are satisfied. First we write the sum in a new form:

$$\sum_G I_G = \exp\left[\sum_p \ln(1+W_p)\right] = \exp\left(\sum_{p'} \frac{W_{p'}}{\tau_{p'}}\right) \tag{4.1}$$

In the second equation the logarithm has been expanded. The prime indicates that the sum now runs over *all* closed paths (including periodic) and $\tau_{p'}$ is the period of path p'. Then the partition sum can be written as[16]

$$Z = \exp\left(E_0 + \sum_{l=0}^{\infty} \frac{1}{2l} \operatorname{Tr} M_l\right) \tag{4.2}$$

with

$$\operatorname{Tr} M_l = \sum_{\mathbf{r}} \sum_{\alpha} \sum_{\beta} M_l(\mathbf{r}, \alpha, \beta; \mathbf{r}, \alpha, \beta) \tag{4.3}$$

and $M_l(\mathbf{r}, \alpha, \beta; \mathbf{r}', \alpha', \beta')$ is the sum of weights of all paths of length l, starting in $\mathbf{r}$, where it arrives from direction α and leaves in direction β and ending in $\mathbf{r}'$, where it arrives from direction α' and leaves in direction β'. The sum in Eq. (4.3) is over all closed paths (also periodic) of length l that can be traced out by a random walker. Therefore M_l can be constructed out of matrices M_2 that describe a double step on the lattice. The advantage of using a two-step matrix M_2 as a basic building block instead of the one-step matrix M_1 is that in using M_2 there are only three directions of arrival and two for leaving, making M_2 a 6×6 matrix, while using M_1, there would be six directions of arrival, giving a 12×12 matrix. (Note that all paths lengths are even.)

In a derivation similar to that given by Feynman,[7] we find for the free energy density

$$f \equiv -\frac{1}{N}\ln(Z)$$

$$= -\sum_i (K_i + L_i + Q_i) - \frac{1}{8\pi^2}\int_0^{2\pi} dq_1 \int_0^{2\pi} dq_2 \ln[\det(I - \Lambda(\mathbf{q}))] \quad (4.4)$$

with Λ the Fourier transform of M_2,

$$\Lambda_{\alpha\beta,\alpha'\beta'}(\mathbf{q}) = \sum_{\mathbf{r}} \exp(i\mathbf{q}\cdot\mathbf{r})\, M_2(\mathbf{o}, \alpha, \beta; \mathbf{r}, \alpha', \beta') \quad (4.5)$$

and I the diagonal matrix. For the matrix Λ we obtain

$$\Lambda_{\alpha\beta,\alpha'\beta'}(\mathbf{q}) = \begin{pmatrix} (\gamma\delta)^{-1}c_3^2 & (\gamma\delta)^{-1}b_1' c_3 \phi^{-1} & 0 & 0 & \gamma^{-1}b_2' b_3' \phi^2 & \gamma^{-1} b_2' c_1 \phi \\ \delta^{-1} b_1' c_2 \phi & \delta^{-1} c_2^2 & \gamma b_2' b_3' \phi^{-2} & \gamma b_3' c_1 \phi^{-1} & 0 & 0 \\ 0 & 0 & \gamma\delta c_3^2 & \gamma\delta b_2' c_3 \phi & \delta b_1' c_2 \phi^{-1} & \delta b_1' b_3' \phi^{-2} \\ \delta^{-1} b_1' b_3' \phi^2 & \delta^{-1} b_3' c_2 \phi & \gamma b_2' c_1 \phi^{-1} & \gamma c_1^2 & 0 & 0 \\ 0 & 0 & \gamma\delta b_1' c_3 \phi & \gamma\delta b_1' b_2' \phi^2 & \delta c_2^2 & \delta b_3' c_2 \phi^{-1} \\ (\gamma\delta)^{-1} b_2' c_3 \phi^{-1} & (\gamma\delta)^{-1} b_1' b_2' \phi^{-2} & 0 & 0 & \gamma^{-1} b_3' c_1 \phi & \gamma^{-1} c_1^2 \end{pmatrix} \quad (4.6)$$

with

$$b_i' = (c_{i+1} c_{i+2})^{1/2} b_i \quad (4.7)$$

$$\gamma = \exp(iq_1) \quad (4.8)$$

$$\delta = \exp(iq_2) \quad (4.9)$$

and $\phi = \exp(-i\pi/6)$ is the phase factor for every counterclockwise turn and ϕ^{-1} for every clockwise turn. These phase factors give to every path p a sign $(-1)^{t_p}$, where t_p is the winding number. Working out the determinant that determines the free energy density, as given by Eq. (4.4), we find

$$\det(I - \Lambda(\mathbf{q})) = \Omega_0^2 + \sum_{j=1}^{3} \Big\{ \Omega_j^2 - 2(\Omega_0 \Omega_j - \Omega_{j+1}\Omega_{j+2}) \cos(q_j) + 4\left(\frac{\Omega_0 - 1}{b_j^2 - 1}\right) \sin^2(q_j) - 4[\Omega_j + c_j^2(\Omega_0 - 2)] \sin(q_{j+1}) \sin(q_{j+2}) \Big\} \quad (4.10)$$

with

$$\Omega_0 = 1 + z_1 z_2 z_3 \tag{4.11}$$

$$\Omega_j = c_j^2(1 + z_j) \tag{4.12}$$

$q_3 = -(q_1 + q_2)$ and z_j is given by Eq. (3.7).

This completes the solution. It is exact only when Eqs. (3.9) and (3.10) hold. But it also provides a good approximation when close encounters are rare, in the important configurations of both the exact and approximate partition sums. So we have a good low-temperature approximation for those phases, for which at least the ground state and its lowest excitations are free of close encounters. We consider this issue only for the isotropic case. Phase A (the phase that has configuration A as the ground state) meets the necessary requirements. For configuration B we can use the symmetries given by Eqs. (1.5)–(1.7) to map it onto configuration A (with anisotropic coupling constants). After the symmetry transformation the free fermion approximation can be applied, and the result will be a good low-temperature approximation (for the free energy) for phase B. So we conclude that in the low-temperature regime, for the isotropic model, the phases A and B are described well. For high temperatures, $b_i \simeq 1$, so that $x_i \simeq 1$ [see Eqs. (3.6) and (3.7)] and the approximation will also be reasonable. For the other parts of the phase diagram, no such regions exist where the approximation is accurate for both high and low temperatures.

For the isotropic model with $K \geqslant 0$ and $L \geqslant Q \geqslant 0$ ($b \geqslant 1$, $z \geqslant 0$) the free fermion conditions obey [see Eq. (3.6)]

$$\prod_{j=1}^{k} x_j' \leqslant (1 + b^4 z)^k$$

$$\leqslant x^k [1 - (1 - x^{-1})(1 - e^{-4K-12Q})]^k \tag{4.14}$$

with x given by Eq. (1.21) and x_j' the close encounter weights as they are dictated by the free fermion conditions, so that

$$1 \leqslant \prod_{j=1}^{k} x_j' \leqslant x^k \tag{4.14}$$

and the approximate partition sum is a strict lower bound.

5. THE CRITICAL SURFACE

The free energy density as given by Eq. (4.4) is analytic unless the determinant given by Eq. (4.10) is zero. In the next section we will show

that for continuous phase transitions q_1, q_2 is 0 or π and Eq. (4.10) becomes

$$\begin{aligned}\det(I-\Lambda(\mathbf{q})) = {} & \delta_{q_1,0}\delta_{q_2,0}(\Omega_0-\Omega_1-\Omega_2-\Omega_3)^2 \\ & + \delta_{q_1,0}\delta_{q_2,\pi}(\Omega_1-\Omega_0-\Omega_2-\Omega_3)^2 \\ & + \delta_{q_1,\pi}\delta_{q_2,0}(\Omega_2-\Omega_0-\Omega_1-\Omega_3)^2 \\ & + \delta_{q_1,\pi}\delta_{q_2,\pi}(\Omega_3-\Omega_0-\Omega_1-\Omega_2)^2 \end{aligned} \tag{5.1}$$

so that the critical surface is given by the condition that the largest Ω is equal to the sum of the three others or

$$\Omega_0+\Omega_1+\Omega_2+\Omega_3 = 2\max(\Omega_0, \Omega_1, \Omega_2, \Omega_3) \tag{5.2}$$

This is the usual form for the critical condition of free fermion models.[17] For the exact free fermion solution, when Eqs. (3.11) and (3.12) hold, Eq. (5.2) reduces to the critical condition for the free fermion solution of the square lattice as derived by Fan and Wu.[6]

Part of the critical surface is clearly an artefact of the approximation. When we set $z_i = -1$ for $i = 1, 2, 3$, all Ω's are zero and Eq. (5.2) is satisfied. But then, according to Eq. (3.6), the weights x_i of close encounters with $\mu_i = \nu_i = 0$ will be zero. So all configurations with close encounters of this type will have their weights reduced to zero. This dramatic effect is solely due to the approximation, since the real weights for these close encounters are always larger than zero.

If, for the isotropic case, we substitute Eqs. (4.11) and (4.12) into the critical condition [Eq. (5.2)] we find for the critical surface

$$1+z = \pm\sqrt{3}\, bc \tag{5.3}$$

(or $z = -1$, which we have already exposed as an artefact of the approximation).

To find the singular behavior of the free energy, we expand it about $q_i = 0, \pi (i = 1, 2)$. For instance, when $q_1 = q_2 = 0$ we have

$$f \sim \int_0 dq_1 \int_0 dq_2 \ln[(\Omega_0-\Omega_1-\Omega_2-\Omega_3)^2 + uq_1^2 + vq_1q_2 + wq_2^2] \tag{5.4}$$

and close to the critical point $(\Omega_0-\Omega_1-\Omega_2-\Omega_3)$ is of $O(T-T_c)$. Performing the integration yields[18]

$$f \sim |T-T_c|^2 \ln|T-T_c| \tag{5.5}$$

and the specific heat will diverge logarithmically unless $(v^2-4uw) \to 0$ as $T \to T_c$; then a different cirtical behavior will be found.

6. THE SURFACE FREE ENERGY

The topological theorem is also valid when an interface contour separating two coexisting phases is present in the system.[11] The interface contour becomes just another path, decoupled from all others. Thus the surface free energy can be calculated between two coexisting phases (one of the phases A–F coexisting with its opposite phase, for which the ground state has all its spins reversed). In the argument below, we specialize to the case of phase A. For the other phases the argument would be analogous.

At $T=0$ a mixed boundary condition, as depicted in Fig. 13, forces the two degenerate ground states to coexist, separated by an interface contour. At $0<T<T_c$ a typical graph will consist of a number of closed paths and an additional interface contour running all the way across the system. The proof of Calheiros *et al.*[11] that the topological theorem can also be applied in this situation is roughly the following. The two bonds on the dual lattice that mark the change from $(+)$ to $(-)$ boundary spins are connected through a new bond (no bend weight at this bond) outside the existing lattice (see Fig. 13). Applying the topological theorem to the lattice with the extra bond gives rise to a new class of closed paths that make use of this bond. All paths that use the new bond more than once cancel each other, leaving as an additional set of paths all random walks starting in $\mathbf{r}=(0,0)$ and ending in $\mathbf{r}'=(m,n)$ (see Fig. 13). Since all paths are decoupled [see Eq. (4.1)] the partition sum Z_{+-} with mixed boundary conditions as in Fig. 13 can be written as

$$Z_{+-}(m,n)=Z_{++}\exp\left(\sum_{p'} W_{p'}\right) \tag{6.1}$$

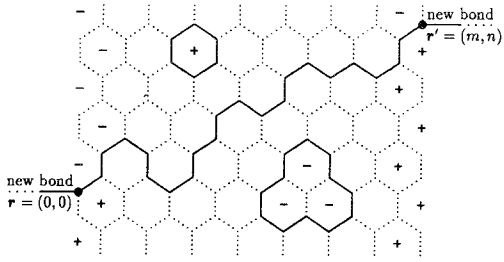

Fig. 13. A typical configuration for the ferromagnetic phase at $0<T<T_c$ when the boundary condition is chosen such that the spin-up phase is forced to coexist with the spin-down phase. An interface contour runs from $\mathbf{r}=(0,0)$ on the left side of the system to $\mathbf{r}'=(m,n)$ on the right side. The average tilt angle θ of the interface is given by $\tan\theta=n/m$. The points $\mathbf{r}$ and $\mathbf{r}'$ are connected through a new bond, of which only the end parts are shown.

with Z_{++} the partition sum with an all (+) boundary. The sum runs over all paths p' (the interface contours) that start in (0, 0) and end in (m, n). Then the surface free energy is[12,13]

$$F_s(m,n) \equiv -\ln\left(\frac{Z_{+-}(m,n)}{Z_{++}}\right) = -\ln\left(\sum_{p'} W_{p'}\right) \tag{6.2}$$

Similar to the way we obtained the bulk free energy, the random walk formalism will give for the angle-dependent free energy density in the thermodynamic limit

$$f_s(\theta) = -\frac{1}{[1+\tan^2(\theta)]^{1/2}} \times \lim_{m\to\infty}\frac{1}{m}\ln\left[\int_0^{2\pi}\frac{dq_1}{2\pi}\int_0^{2\pi}\frac{dq_2}{2\pi}\int_0^{2\pi}\frac{dq_2}{2\pi}\exp(-i\mathbf{q}\cdot\mathbf{r})\,\mathrm{Tr}(I-\Lambda(\mathbf{q}))^{-1}\right] \tag{6.3}$$

with $\mathbf{r} = (m, n)$ and $\tan(\theta) = n/m$. This expression can be evaluated with the steepest descent method. Note that the saddle point does not change (in the thermodynamic limit) when $\mathrm{Tr}(I-\Lambda(\mathbf{q}))^{-1}$ is replaced by $[\det(I-\Lambda(\mathbf{q}))]^{-1}$ because

$$\mathrm{Tr}(I-\Lambda(\mathbf{q}))^{-1} = \sum_{i=1}^{6}(1-\lambda_i)^{-1} = \frac{c(\mathbf{q})}{\det(I-\Lambda(\mathbf{q}))} \tag{6.4}$$

with λ_i the eigenvalues of the matrix Λ and

$$c(\mathbf{q}) = \sum_{i=1}^{6}\prod_{j\neq i}(1-\lambda_j(\mathbf{q})) \tag{6.5}$$

which is harmless at the saddle point. The steepest descent method yields[13]

$$f_s(\theta) = k_1\cos(\theta) + k_2\sin(\theta) \tag{6.6}$$

with

$$\begin{aligned} k_1 &= -i[q_1(\mathrm{mod}\,\pi)] \\ k_2 &= -i[q_2(\mathrm{mod}\,\pi)] \end{aligned} \tag{6.7}$$

where $\mathbf{q}$ is the solution of $\det(I-\Lambda(\mathbf{q})) = 0$ ($\mathbf{q}$ is purely imaginary) and

$$\tan(\theta) = \frac{\partial_{q_1}\det(I-\Lambda(\mathbf{q}))}{\partial_{q_2}\det(I-\Lambda(\mathbf{q}))} \tag{6.8}$$

Note that the determinant that gives the bulk partition sum also completely determines the angle-dependent free energy density.

For a continuous transition, $f_s \to 0$ as $T \to T_c$. Therefore $k_1, k_2 \to 0$, which justifies putting q_1, q_2 equal to 0 or π in our search for the critical surface.

Finally, we remark that the equilibrium crystal shape can be obtained as a Legendre transformation of the surface free energy.[12,13] If $Y(X)$ is the equilibrium crystal shape in Cartesian coordinates, then

$$X = \lambda k_x \tag{6.9}$$

$$Y = \lambda k_y \tag{6.10}$$

with k_x and k_y given by Eq. (6.7) and λ a constant controlling the volume of the crystal.

7. SUMMARY

We have derived an approximate expression for the partition function of an Ising model on a triangular lattice with further-neighbor interactions by extending the method of Vdovichenko, which is based on an equivalence between a summation over graphs and a summation over products of unrestricted paths with only local weights. The equivalence is exact only when the free fermion conditions are satisfied and is approximate outside the free fermion region. For the general solution, the path sum gives approximate weights to the close encounters in the graphs. Outside the free fermion region, the close encounter weights so generated depend on the configuration and cannot be seen as a local shift of the x_i.

The approximation will be accurate when close encounters are rare. We have found these regions by deriving the zero-temperature phase diagram for isotropic coupling constants. We find that in phase A and phase B [through the symmetry transformations (1.5)–(1.7)] close encounters are absent in the ground state and in the lowest excitations (see Fig. 6). So we conclude that the phases A and B are well described in the low-temperature phase by the free fermion approximation for the free energy.

On the basis of this free energy we have calculated the critical surface and the surface free energy for the corresponding coexisting phases, using the extension of Vdovichenko's method by Calheiros *et al.* In addition, we have determined the equilibrium crystal shapes.

APPENDIX A. CONSISTENCY RELATIONS BETWEEN THE NUMBERS OF VERTEX PAIRS

What are the relations between the numbers of vertex pairs $n_i(q)$ for an arbitrary configuration of the system? First, the total number of vertex pairs with orientation i is given by the total number of sites

$$\sum_{q=1}^{8} n_i(q) = N \tag{A.1}$$

Next, note that every bond or hole is part of five different vertex pairs. We assign a fraction f_j of the bond (hole) to each of them, so that the bond (hole) becomes distributed over these five vertex pairs. The most general distribution is shown in Fig. 14, together with the condition that

$$\sum_{j=0}^{4} f_j = 1 \tag{A.2}$$

The total number of bonds N_i^b with orientation i for an arbitrary configuration is given by

$$\begin{aligned} N_i^b = {} & f_0(n_i(3) + n_i(4) + n_i(5) + n_i(6) \\ & + f_1(n_{i+2}(2) + n_{i+2}(3) + n_{i+2}(5) + n_{i+2}(7)) \\ & + f_2(n_{i+1}(2) + n_{i+1}(4) + n_{i+1}(6) + n_{i+1}(7)) \\ & f_3(n_{i+2}(2) + n_{i+2}(3) + n_{i+2}(6) + n_{i+2}(8)) \\ & + f_4(n_{i+1}(2) + n_{i+1}(4) + n_{i+1}(5) + n_{i+1}(8)) \end{aligned} \tag{A.3}$$

If we choose two different distributions f_j and f_j' and subtract the resulting expressions for N_i^b, we obtain the following consistency relation between the numbers n_q:

$$\sum_{j=0}^{4} \Delta f_j s_{j,i} = 0 \tag{A.4}$$

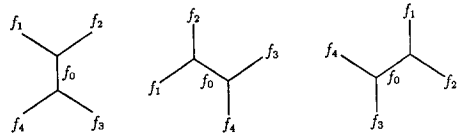

Fig. 14. For the vertex pairs, the fractions f_i of the bonds that are assigned to it are indicated. A bond is part of five different vertex pairs and the sum of the fractions of the bond assigned to each of these vertex pairs is 1.

with

$$s_{0,i} = n_i(3) + n_i(4) + n_i(5) + n_i(6) \tag{A.5}$$

$$s_{1,i} = n_{i+2}(2) + n_{i+2}(3) + n_{i+2}(5) + n_{i+2}(7) \tag{A.6}$$

$$s_{2,i} = n_{i+1}(2) + n_{i+1}(4) + n_{i+1}(6) + n_{i+1}(7) \tag{A.7}$$

$$s_{3,i} = n_{i+2}(2) + n_{i+2}(3) + n_{i+2}(6) + n_{i+2}(8) \tag{A.8}$$

$$s_{4,i} = n_{i+1}(2) + n_{i+1}(4) + n_{i+1}(5) + n_{i+1}(8) \tag{A.9}$$

and

$$\Delta f_j = f_j - f'_j, \qquad j = 0, \ldots, 4 \tag{A.10}$$

while the condition (A.2) becomes

$$\sum_{j=0}^{4} \Delta f_j = 0 \tag{A.11}$$

We can use eq. (A.11) to eliminate one of the variables Δf_j in favour of the others in Eq. (A.4) so that the remaining Δf_j are independent and we find the solution

$$s_{0,i} = s_{1,i} = s_{2,i} = s_{3,i} = s_{4,i} \tag{A.12}$$

or equivalently

$$n_i(5) = n_i(6) \tag{A.13}$$

$$n_i(7) = n_i(8) \tag{A.14}$$

$$n_i(2) + n_i(7) = n_{i+1}(3) + n_{i+1}(5) = n_{i+2}(4) + n_{i+2}(5) \tag{A.15}$$

In Eqs. (A.1) and (A.13)–(A.15) we have a total of 15 independent relations between the numbers $n_i(q)$. With these, the partition sum given by Eq. (1.3) can be rewritten in the form of Eq. (1.8) by eliminating $n_i(1)$, $n_i(3)$, and $n_i(4)$ in favor of $n_i(2)$, $n_i(5) + n_i(6)$, and $n_i(7) + n_i(8)$, leaving only $24 - 15 = 9$ independent variables: a_i, b_i, and c_i.

In Section 2 we need the relations between the numbers of vertex pairs for the isotropic case where $a_i = a$, $b_i = b$, and $c_i = c$ for $i = 1, 2, 3$. Summing Eq. (A.1) and (A.13)–(A.15) over i, we obtain the consistency relations for the isotropic case:

$$\sum_{q=1}^{8} n(q) = 3N \tag{A.16}$$

$$n(3) = n(4) \tag{A.17}$$

$$n(5) = n(6) \tag{A.18}$$

$$n(7) = n(8) \tag{A.19}$$

$$2n(2) + n(7) + n(8) = n(3) + n(4) + n(5) + n(6) \tag{A.20}$$

APPENDIX B. THE GROUND STATES

We restrict ourselves to the isotropic case and set $a_i = a$, $b_i = b$, and $c_i = c$ (or $K_i = K$, $L_i = L$, and $Q_i = Q$) for $i = 1, 2, 3$. In Fig. 6 we show six configurations A–F that are likely candidates for the ground states. Assuming that these configurations are all the possible ground states, Figs. 7 and 8 give the zero-temperature phase diagrams for $Q > 0$ and $Q < 0$, respectively. Let us now try to prove the correctness of these phase diagrams. The argument consists of three parts. In the first part we try to establish the zero-temperature phase diagram, using the consistency relations between the numbers of vertex pairs as derived in Appendix A. The consistency relations take into account the connectivity properties of the vertex pairs only to some extent. They are nessessary but not sufficient conditions for the existence of a configuration. For this reason, for the ground states B, E, and F, the proof turns out to be incomplete. In the second part we employ a different strategy, which proves to be useful for establishing the ground states B and E. For this, consider all possible configurations on a hexagon (see Fig. 15). Note that for configurations B and E in Fig. 6 every hexagonal part of the lattice is in the same configuration (apart from symmetry). If this hexagonal configuration has a lower energy then all others, the corresponding configuration B or E is the ground state. With this additional argument, the complete zero-temperature phase diagram can be found, except for the region in Fig. 8 where configuration F is assumed to be the ground state. In the last part it will be made plausible

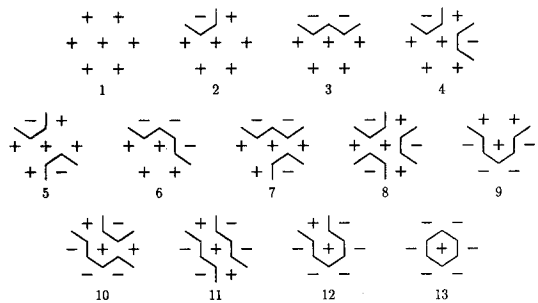

Fig. 15. All possible configurations on a hexagon (apart from symmetry).

(but not proven) that configuration F is indeed the ground state for this last region.

In the first part, all we need are the consistency relations and an expression for the weight of a configuration. In Appendix A we have derived that for every configuration the numbers of vertex pairs $n(q) = \sum_i n_i(q)$ must obey the relations

$$\sum_{q=1}^{8} n(q) = 3N \tag{B.1}$$

and

$$2n(2) + n(7) + n(8) = n(3) + n(4) + n(5) + n(6) \tag{B.2}$$

Summing them, we get

$$n(1) + 3n(2) + 2[n(7) + n(8)] = 3N \tag{B.3}$$

From the expression for the partition sum given by Eq. (1.8), together with the definition (1.14), we see that the weight W of a configuration is proportional to

$$W \sim (cx^{1/2})^{2n(2)} b^{n(5)+n(6)} c^{n(7)+n(8)} 1^{n(1)+n(3)+n(4)} \tag{B.4}$$

For every point of the phase diagram, we will have to look for the values of $n(2)$, $n(5)+n(6)$, $n(7)+n(8)$, and $n(1)+n(3)+n(4)$ that will maximize the weight W, given the restrictions posed by the consistency relations. Since the consistency relations are not sufficient to imply the existence of a configuration, we will end by examining the realizability of the proposed solutions.

Because $W \sim 1^{n(3)+n(4)} b^{n(5)+n(6)}$, while for the consistency relations only the total sum $n(3)+n(4)+n(5)+n(6)$ is relevant and not how the total sum is broken up into $n(3)+n(4)$ and $n(5)+n(6)$, it is favorable to set $n(3)+n(4)=0$ if $b>1$, and to set $n(5)+n(6)=0$ if $b<1$. First consider the case $b>1$ and put $n(3)+n(4)=0$. Then we can eliminate $n(5)+n(6)$ in favor of $n(2)$ and $n(7)+n(8)$, using Eq. (B.2), and we have

$$W \sim (bcx^{1/2})^{2n(2)} (bc)^{n(7)+n(8)} 1^{n(1)} \tag{B.5}$$

To decide which state will be the ground state we consider all possible orderings of the weights $bcx^{1/2}$, bc, and 1, thereby subdividing case $b>1$ into the following four subcases:

(i) $1 > bc$, $bcx^{1/2}$: Then the maximum weight is obtained when $n(1) = 3N$ and all other $n(q)$'s are zero.

(ii) $bcx^{1/2} > bc$, 1: In this case we have to maximize $n(2)$. According to Eq. (B.3), $n(2) \leqslant N$ and $n(2) = N$ only when $n(1) = n(7) + n(8) = 0$. Substituting this into Eq. (B.2), we see that $n(5) + n(6) = 2N$ [remember we put $n(3) + n(4) = 0$]. The only way to improve on this might be by making $n(7) + n(8) > 0$ for $bc > 1$. But note that increasing $n(7) + n(8)$ means decreasing $n(2)$ [see Eq. (B.3)] and at best we can exchange two vertex pairs of type $q = 2$ for three vertex pairs of type $q = 7, 8$, which would make the weight of the configuration lower. Thus $n(2) = N$, $n(5) + n(6) = 2N$, and all other $n(q)$'s zero gives the largest weight W for this case.

(iii) $bc > 1 > bcx^{1/2}$: In this case we must maximize $n(7) + n(8)$ and minimize $n(2)$. So we have $n(7) + n(8) = 3N/2$ and $n(2) = 0$ [see Eq. (B.3)]. Substituting this into Eq. (B.2), we see that $n(5) + n(6) = 3N/2$. Thus, having $n(5) + n(6) = n(7) + n(8) = 3N/2$ and all other $n(q)$'s zero, the weight W obtains its largest value.

(iv) $bc > bcx^{1/2} > 1$: Again $n(5) + n(6) = n(7) + n(8) = 3N/2$ is a good option. Improvement is possible only by making $n(2) > 0$, although it makes $n(7) + n(8) < 3N/2$. From Eq. (B.3) we see that we can exchange three vertex pairs of type $q = 7, 8$ for two vertex pairs of type $q = 2$. If this increases the weight W [when $(bcx^{1/2})^4 > (bc)^3$, that is, when $bcx^2 > 1$] we should eliminate all vertex pairs of type $q = 7, 8$ in this way, obtaining $n(2) = N$ and $n(5) + n(6) = 2N$. Thus, for $bcx^2 < 1$, we should take $n(5) + n(6) = n(7) + n(8) = 3N/2$, while for $bcx^2 > 1$, it is better to have $n(2) = N$ and $n(5) + n(6) = 2N$.

Next consider the case $b < 1$ and put $n(5) + n(6) = 0$. Then the weight W becomes

$$W \sim (cx^{1/2})^{2n(2)} (c)^{n(7)+n(8)} 1^{n(1)+n(3)+n(4)} \tag{B.6}$$

Note that the weight W has the same form as Eq. (B.5), except that the factors b are missing, and that the consistency relations are unchanged, except that $n(5) + n(6)$ is replaced by $n(3) + n(4)$. Thus, analogous to the case $b > 1$, the weight W obtains its maximum value as follows:

(v) $1 > c$, $cx^{1/2}$: $n(1) = 3N$.

(vi) $cx^{1/2} > c$, 1: $n(2) = N$ and $n(3) + n(4) = 2N$.

(vii) $c > 1 > cx^{1/2}$: $n(3) + n(4) = n(7) + n(8) = 3N/2$.

(viii) $c > cx^{1/2} > 1$: $n(3) + n(4) = n(7) + n(8) = 3N/2$ for $cx^2 < 1$ and $n(2) = N$ and $n(3) + n(4) = 2N$ for $cx^2 < 1$.

If all the optimal solutions would correspond to one of the six configurations A–F as given in Fig. 6, we would be done. But remember that the consistency relations to not imply the existence of a configuration. So it is

not even clear that the solutions found for the above cases (i)–(viii) are actually realizable. Inspecting Fig. 6, we see that the solutions for the cases (i)–(vi) are realized by configuration A, B, C, or D. For case (vii) we found that the weight W reaches its maximum value when $n(3)+n(4)=n(7)+n(8)=3N/2$. This turns out not to be possible, as will be proven in the last part of this appendix. There we show that, if we are to avoid vertex pairs of type $q=1, 2$ [$n(1)=n(2)=0$, so that, according to Eqs. (B.2) and (B.3), $n(7)+n(8)=n(3)+n(4)+n(5)+n(6)=3N/2$], the maximum for $n(3)+n(4)$ is only $N/2$. So it is not clear which state will be the ground state here. For case (viii) the ground state is configuration B if $cx^2>1$, but if $bx^2<1$, we stumble over the same problem as in case (vii).

The dotted lines in Figs. 7 and 8 mark the regions that belong to case (vii) and case (viii) for $cx^2>1$, the parts of the phase diagrams for which the ground states are still unknown. In this second part of our argument we will prove the correctness of these parts of these phase diagrams as far as configurations B and E are concerned. Consider all possible configurations on a hexagon (see Fig. 15) and write the weight of a configuration of the system as a product of hexagon weights. Each site of the lattice will act as the central site of a hexagon. In this way every diamond (or vertex pair) will be counted twice, so to each hexagon we will assign only half of its energy. There are only 13 different configurations possible on the hexagon (apart from symmetry), as shown in Fig. 15. The hexagon energy could be taken equal to the sum of the six diamonds that are present in it. Then there is no contribution from the K-interactions between the spins that lie on the boundary of the hexagon. To make the distribution of the total energy over the hexagons adjustable, we prefer to count the contribution of the K-interactions between the boundary spins for a fraction f, and the contribution of the K-interactions that involve the central spin of the hexagon for a fraction $1-f$ $(0\leqslant f\leqslant 1)$. The hexagon energy ε_h is then given by

$$\varepsilon_h=-\frac{1}{2}\Bigg\{K\sum_{j=1}^{6}[f\sigma_j\sigma_{j+1}+(1-f)\sigma_0\sigma_j]+L\sum_{j=1}^{6}\sigma_j\sigma_{j+2}+Q\sum_{j=1}^{6}\sigma_0\sigma_j\sigma_{j+1}\sigma_{j+2}\Bigg\} \tag{B.7}$$

We list the hexagon energies ε_h in Table I together with the ground states in which these hexagons are present.

If we choose $f=2/3$, hexagon configuration 3 has the lowest energy in the entire region assigned to configuration E in both the phase diagrams of Figs. 7 and 8. This proves that it is the correct ground state for this region. Next consider the two regions where configuration B is assumed to be the

Table I. Hexagon Configurations and Their Weights

Hexagon configuration	ε_h	Ground state
1	$-(3K+3L+3Q)$	A
2	$-(2-f)K-L$	
3	$-K+L-Q$	E
4	$-(1-2f)K-L+Q$	
5	$-(1-2f)K+L+3Q$	D, F
6	$-fK+L$	
7	$fK+L$	
8	$-3(fK+L)$	C
9	$(1-2f)K+L+Q$	F
10	$K-L-Q$	
11	$K+L-3Q$	B
12	$(2-3f)K-L$	
13	$3(1-2f)K-3L+3Q$	C, D

ground state. Both regions are divided into two parts by the dotted lines. We are concerned with the parts where it has not yet been proved that configuration B is the ground state. If we choose $f=1/3$ (when $Q>0$) and $f=2/5$ (when $Q<0$), we find that hexagon configuration 11 has the lowest energy for these parts. Thus, configuration B is the ground state in the whole region assigned to it in Figs. 7 and 8.

What remains is whether configuration F is correctly assigned in Fig. 8. This we can make plausible but not prove (since configuration F consists of two types of hexagon configurations, we cannot use the same arguments as we used for configurations B and E above). If we consider only the configurations that can be constructed out of the last six vertex pairs of Fig. 3, then, among these, configuration F is the state with the lowest energy in this last region. For then, only hexagon configurations 5, 9, and 11 can occur and all possible states are obtained from stacking the rows R and R' as shown in Fig. 16. Thus, only two possible ground states can be constructed. If row R has a lower energy than row R', we should use only row R and we obtain configuration F, and if row R' has the lowest energy, we stack only row R' and we obtain configuration D. In this last region, row R has the lowest energy, so that configuration F is the best candidate for the ground state. Since configuration F also has a larger energy than configurations B and E here, the first two vertex pairs are probably not so important in this part of the phase diagram.

Finally, note that $n(3)+n(4)=0$ for row R'. Therefore, if $n(1)=n(2)=0$, $n(3)+n(4)$ reaches its maximum value in configuration F, where it is $N/2$, as was stated in the first part of our argument.

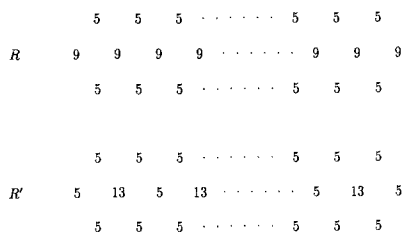

Fig. 16. Two rows R and R' each of which consists of three layers of overlapping hexagons. The numbers refer to the hexagon configurations in Fig. 15.

APPENDIX C. THE TOPOLOGICAL THEOREM

In this appendix we consider to what extent the terms generated by expanding the rhs of Eq. (3.1), cancel. We will follow the arguments given by Burgoyne[16] for the nearest neighbor Ising model on a square lattice. Apart from the difference in lattices (ours is hexagonal), we have the complication that the bend weights $b_i \neq 1$. We will not repeat the complete proof by Burgoyne, but indicate only where slight modifications are needed.

First it is proved that the terms of the rhs with only single bonds add up to $\sum I_G$. Since we work on a hexagonal lattice, there are no crossings (which means no complications with different path interpretations for a crossing as one has for the square lattice) and the statement is trivially true.

Next consider all terms on the rhs which have overlapping bonds. Group together the terms that have the same bonds the same number of times. Consider one such group and choose an N-fold bond ($N \geqslant 2$). Remove this N-fold bond so that each terms of the group is a product of closed paths and a set of N path segments. The terms leading to the same path segments are collected in subgroups. For the nearest neighbor Ising model the terms within each subgroup cancel each other. This is proved by induction. First it is shown that for a subgroup for which all path segments are *different*, the terms cancel. Second it is shown that if the terms within a subgroup cancel, then replacing one path segment (different from all others) by a path segment already present results in a new subgroup (with less terms because not every way of connecting the path segments gives an existing term) that also cancels.

For the first part of the proof consider a subgroup for which all path segments are different. Every way of connecting the segments (that is, each term) corresponds to a permutation π that specifies which of the N neighbor bonds on one side of the N-fold bond is connected to which one

on the other side. If the permutation is un(even), then the number of crossings at the N-fold bond is un(even). For the nearest neighbor Ising model the absolute weights of all the terms of the subgroup are equal, while their sign depends on the sign (even or uneven) of the permutation. Because half the permutations are un(even), the sum of the terms is zero. In our case not all the terms have the same absolute weight, because $b_i \neq 1$ (see Fig. 9). But when two neighbor bonds on the same side of the N-fold bond are parallel (say bond numbers i and j), then the terms corresponding to the permutations π and $\pi' = (\pi_i, \pi_j) \circ \pi$, cancel. Here (π_i, π_j) is a transposition of π_i and π_j. When $N \geqslant 3$ there are always two parallel neighbor bonds. So, only when $N = 2$ and the configuration of the neighboring bonds is as in Fig. 9 will there be no cancellation.

In the second part of the proof, the cancellation of the terms within a subgroup where some of the segments are equal is derived from the cancellation of a subgroup where one of those equal segments (say q_1) is replaced by one (say q_0) that is different from all others. If q_0 is chosen such that the two terminal bonds (the bonds that border on the N-fold bond) are equal to the terminal bonds of q_1, this second part of the proof remains valid in our case. Note that the terms that did not cancel in the first part of the proof do not impair the induction process, since they are not needed in the second part (because there are no terms with just two equal path segments).

ACKNOWLEDGMENTS

Part of this research was supported by the Stichting voor Fundamenteel Onderzoek der Materie (FOM), which is financially supported by the Nederlandse Organisatie voor Wetenschappelijk Onderzoek (ZWO).

REFERENCES

1. L. Onsager, *Phys. Rev.* **65**:117 (1944).
2. L. J. de Jongh and A. R. Miedema, *Experiments on Simple Magnetic Model Systems* (Taylor and Francis, London, 1974).
3. B. Widom, *J. Chem. Phys.* **84**:6943 (1986).
4. M. Schick and W. Shih, *Phys. Rev. B* **34**:1797 (1986).
5. C. A. Hurst and H. S. Green, *J. Chem. Phys.* **33**:1059 (1960); C. A. Hurst, *J. Math. Phys.* **7**:305 (1966).
6. C. Fan and F. Y. Wu, *Phys. Rev.* **179**:560 (1969); *Phys. Rev. B* **2**:723 (1970).
7. R. P. Feynman, *Statistical Mechanics* (Benjamin|Cummings, Reading, Massachusetts, 1972), pp. 136–150.
8. N. V. Vdovichenko, *Zh. Eksp. Teor. Fiz.* **47**:715 (1964) [*Sov. Phys. JETP* **20**:477 (1965)].
9. G. V. Ryazanov, *Zh. Eksp. Teor. Fiz.* **59**:1000 (1970) [*Sov. Phys. JETP* **32**:544 (1971)].

10. F. Wiegel, *Phys. Lett.* **41A**:225 (1972).
11. F. Calheiros, S. Johannesen, and D. Merlini, *J. Phys. A* **20**:5991 (1987).
12. M. Holzer, *Phys. Rev. Lett.* **64**:653 (1990); *Phys. Rev. B* **42**:10570 (1990).
13. Y. Akutsu and N. Akutsu, *Phys. Rev. Lett.* **64**:1189 (1990).
14. F. Y. Wu, *J. Math. Phys.* **15**:687 (1974).
15. S. Sherman, *J. Math. Phys.* **1**:202 (1960); *J. Math. Phys.* **4**:1213 (1963).
16. P. N. Burgoyne, *J. Math. Phys.* **4**:1320 (1963).
17. J. E. Sacco and F. Y. Wu, *J. Phys. A* **8**:1780 (1975).
18. C. S. Hsue, K. Y. Lin, and F. Y. Wu, *Phys. Rev. B* **12**:429 (1975).